A New Type of Thermally Induced Spin Transition Associated with an Equatorial ↔ Axial Conversion in a Copper(II)–Nitroxide Cluster

Fabrice Lanfranc de Panthou,[†] Elie Belorizky,[‡] Roberto Calemczuk,[§] Dominique Luneau,[†] Christophe Marcenat,[§] Eric Ressouche,[§] Philippe Turek,[⊥] and Paul Rey*,[†]

Contribution from CNRS-Laboratoire de Chimie de Coordination (URA 1194), CEA-Département de Recherche Fondamentale sur la Matière Condensée, Centre d'Etudes Nucléaires de Grenoble, SESAM and SPSMS, 17 rue des Martyrs, 38054 Grenoble Cedex 09, France, the Laboratoire de Spectrométrie Physique (associé au CNRS), Université Joseph Fourier, BP 87, 38402 Saint-Martin-d'Hères Cedex, France, and Institut Charles Sadron, 6 rue Boussingault, 67083 Strasbourg, France

Received July 24, 1995[⊗]

Abstract: The nitroxide free radical 2-(3-pyridyl)-4,4,5,5-tetramethyl-4,5-dihydro-1*H*-imidazolyl-1-oxy-3-oxide (L) reacts with $Cu(hfac)_2$, leading to a complex of formula $[Cu(hfac)_2]_4L_2$. This complex has a cyclic molecular structure where two copper ions are bridged by the free radicals. The two remaining metal centers are extracyclic. Both oxygen atoms of the nitronyl nitroxide ligand are axially bound to both types of copper(II) ions at room temperature while, at 50 K, coordination of the NO group to the intracyclic metal ion is equatorial. The magnetic behavior is strongly correlated to the change of coordination. While at room temperature one observes a Curie law corresponding to six independent $S = 1/2$ spins, at low temperature only two $S = 1/2$ spins are observed. This behavior is rationalized in the frame of the dependence of the metal–ligand exchange interaction upon the coordination geometry in nitroxide–copper derivatives. This spin transition is further characterized by EPR spectroscopy and heat capacity measurements. Relevant structural parameters at room temperature are as follows: space group $P\bar{1}$, $a = 11.509(2)$ Å, $b = 12.673(2)$ Å, $c = 16.077(2)$ Å, $\alpha = 70.29(1)°$, $\beta = 81.29(1)°$, $\gamma = 84.68(1)°$, $Z = 2$.

Although much of their popularity stems from their use as spin probes in biological systems,[1-5] nitroxide free radicals are now attracting much interest as spin carriers in the design of molecular magnetic materials.[6-13] In particular, considerable attention has been devoted to their coordination chemistry and to the magnetic properties of their metal complexes.[9-13]

Copper(II)–nitroxide magnetochemistry is especially well documented and characterized by versatile magnetic behaviors which depend on coordination geometry.[10-19] When the free radical ligand is axially bound by the oxygen atom to a square pyramidal or octahedral metal ion, the $S = 1/2$ spins are weakly and ferromagnetically coupled.[11-17] In contrast, an equatorial binding results in a strong antiferromagnetic metal-free radical coupling.[13,18,19] Although coordination preference is difficult to predict, a few guidelines have emerged on examining the numerous reported examples. Thus, the chemical structure of the free radical ligand plays a major role as observed in complexes of multidentate nitroxide ligands which coordinate axially. In contrast, when the nitroxyl group is the only active coordination site, equatorially bonded species are generally obtained.[10] These facts have been rationalized as follows: (i) considering only the nitroxyl group, equatorial binding is preferred because spin pairing is a stabilizing factor. (ii) The presence of several coordination sites and metal centers leads to axially bound species, steric factors being the main cause of geometry change. In addition, one must take into account intermolecular interactions in the solid state such as those occurring between uncoordinated nitroxyl groups in some copper(II) derivatives of nitronyl nitroxides. Thus, coordination geometry results from a delicate balance between numerous and uncontrolled factors, and it is expected that in some of these species the energy gap between equatorial and axial coordination is very weak.

[†] SESAM.
[‡] Université Joseph Fourier.
[§] SPSMS.
[⊥] Institut Charles Sadron.
[⊗] Abstract published in *Advance ACS Abstracts,* October 15, 1995.

(1) Stone, T. J.; Buckman, T.; Nordio, P. L.; McConnell, H. M. *Proc. Natl. Acad. Sci. U.S.A.* **1965**, *54*, 1010.
(2) Hamilton, C. L.; McConnell, H. M. In *Structural Chemistry and Molecular Biology*; Rich, A., Davidson, N., Eds.; W. H. Freeman: San Francisco, 1968; p 115.
(3) Griffith, O. H.; Waggoner, A. S. *Acc. Chem. Res.* **1969**, *2*, 17.
(4) McConnell, H. M.; McFarland, B. G. *Q. Rev. Biophys.* **1970**, *3*, 21.
(5) Eaton, S. S.; Eaton, G. R. *Coord. Chem. Rev.* **1978**, *26*, 207.
(6) Turek, P.; Nozawa, K.; Shiomi, D.; Awaga, K.; Inabe, T.; Maruyama, Y.; Kinoshita, M. *Chem. Phys. Lett.* **1991**, *180*, 327.
(7) Chiarelli, R.; Novak, M. A.; Rassat, A.; Tholence, J.-L. *Nature* **1993**, *363*, 147.
(8) Cirujeda, J.; Mas, M.; Molins, E.; Lanfranc de Panthou, F.; Laugier, J.; Park, J. G.; Paulsen, C.; Rey, P.; Rovira, C.; Veciana, J. *J. Chem. Soc., Chem. Commun.* **1995**, 709.
(9) Beck, W.; Schmidtner, K.; Keller, H. J. *Chem. Ber.* **1967**, *100*, 503.
(10) Dickman, M. H.; Doedens, R. J. *Inorg. Chem.* **1981**, *20*, 2677.
(11) Anderson, O. P.; Kuechler, T. C. *Inorg. Chem.* **1980**, *19*, 1417.
(12) Caneschi, A.; Gatteschi, D.; Sessoli, R.; Rey, P. *Acc. Chem. Res.* **1989**, *22*, 392.
(13) Caneschi, A.; Gatteschi, D.; Rey, P. *Prog. Inorg. Chem.* **1991**, *39*, 331.
(14) Bencini, A.; Benelli, C.; Gatteschi, D.; Zanchini, C. *J. Am. Chem. Soc.* **1984**, *106*, 5813.
(15) Grand, A.; Rey, P.; Subra, R. *Inorg. Chem.* **1983**, *22*, 391.
(16) Caneschi, A.; Gatteschi, D.; Laugier, J.; Rey, P. *J. Am. Chem. Soc.* **1987**, *109*, 2191.
(17) Caneschi, A.; Gatteschi, D.; Grand, A.; Laugier, J.; Pardi, L.; Rey, P. *Inorg. Chem.* **1988**, *27*, 1031.
(18) Laugier, J.; Rey, P.; Benelli, C.; Gatteschi, D.; Zanchini, C. *J. Am. Chem. Soc.* **1986**, *108*, 6931.
(19) Gatteschi, D.; Laugier, J.; Rey, P.; Zanchini, C. *Inorg. Chem.* **1987**, *26*, 938.

0002-7863/95/1517-11247$09.00/0

We describe herein such an example of a nitronyl nitroxide–copper(II) complex where the coordination of the free radical ligand converts from axial to equatorial on decreasing the temperature. As a consequence, the temperature dependence of the magnetic susceptibility exhibits a discontinuity phenomenologically similar to that observed for first-row transition-metal complexes undergoing a spin-crossover transition.

The nature of the transition has been characterized by magnetic susceptibility measurements, low- and room-temperature crystal structure determinations, EPR spectroscopy, and specific heat measurements. These studies afford evidence that structural and magnetic changes are correlated and that the conversion is entropy driven. This copper(II)–nitroxide cluster is the first representative of a family of compounds undergoing a spin transition involving several spin carriers.

Experimental Section

Syntheses. 2-(3-Pyridyl)-4,4,5,5-tetramethyl-4,5-dihydro-1*H*-imidazolyl-1-oxy-3-oxide (NIT-3Py)[20] and anhydrous bis(hexafluoroacetylacetonato)copper(II) (Cu(hfac)$_2$)[21] were prepared as previously reported.

Bis[(2-(3-pyridyl)-4,4,5,5-tetramethyl-4,5-dihydro-1*H*-imidazolyl-1-oxy-3-oxide)–bis[bis(hexafluoroacetylacetonato)copper(II)]], {[Cu(hfac)$_2$]$_2$(NIT-3PY)}$_2$, was prepared as follows: To a solution of Cu(hfac)$_2$ (960 mg, 2 × 10^{-3} M) in warm (70 °C) heptane (100 mL) was added with stirring a solution of NIT-3Py (237 mg, 10^{-3} M) in chloroform (5 mL). The solution was stirred for an additional 15 min and allowed to cool to room temperature in the dark. After 1 h the solution was filtered, and the filtrate was kept for 12 h at 4 °C. The crystals which formed (882 mg, 74%, mp 118 °C) were filtered and vacuum dried. Anal. Calcd for $C_{32}H_{18}F_{24}N_3O_{10}Cu_2$: C, 32.29; H, 1.70; F, 38.34; N, 3.53; O, 13.45; Cu, 10.69. Found: C, 32.30; H, 2.01; F, 37.92; N, 3.64; Cu, 10.72.

Magnetic and EPR Measurements. Magnetic data were collected by use of a superconducting Quantum Design SQUID magnetometer working at a 0.5 T field strength in the 2–300 K temperature range. The SQUID outputs were corrected for the magnetization of the sample holder, and the magnetic susceptibilities were corrected for the diamagnetism of the constituent atoms using Pascal constants.

EPR experiments were performed on a Bruker ER-200 spectrometer operating at 9.3 GHz. The rectangular TE102 cavity was equipped with an Oxford continuous-flow cryostat for low-temperature data recording. A single crystal of the compound was oriented on an automatic Laue apparatus[22] attached with Apiezon grease to a Teflon sample holder and inserted into a quartz tube which was sealed under He partial pressure ($P \cong 20$ mmHg). To this assembly was attached a thermocouple for precise control of the temperature. It proved difficult to bring a crystal to low temperature without breaking. Thus, only one orientation corresponding to the rotation of the magnetic field in the $\vec{b}-\vec{a},\vec{c}$ plane could be successfully studied down to 4.2 K.

Room Temperature Data Collection and Structure Determination. Preliminary Wiessenberg photographs showed the triclinic system. A crystal of approximate dimensions 0.2 × 0.2 × 0.2 mm^3 was mounted on an Enraf-Nonius CAD-4 four-circle diffractometer equipped with graphite-monochromatized Mo Kα radiation. Accurate cell constants were obtained from least-squares fitting of the setting angles of 25 reflections. They are reported in Table 1 with pertinent details regarding the determination of the structure. The intensities of 8678 reflections, among which 2636 had $|F| > 3\sigma|F|$, were measured with an ω scan and corrected for Lorentz and polarization factors but not for absorption.

The initial choice of the $P\bar{1}$ space group was fully confirmed by all subsequent developments during the structure determination. Using direct methods included in the SHELLX86 package,[23] most of the non-hydrogen atoms were observed. Then, difference Fourier maps revealed electron density appropriately located for the missing heavy atoms. These were refined in the anisotropic approximation using a full-matrix least-squares procedure. In the final refinement model, hydrogen atoms were included in calculated and fixed positions with isotropic thermal parameters equal to those of the connected carbon atoms.

Table 1. Crystallographic Data for {[Cu(hfac)$_2$]$_2$(NIT-3Py)}$_2$

chemical formula	$C_{64}H_{36}Cu_4F_{48}N_6O_{20}$		
formula weight	2375.2		
space group	$P\bar{1}$		
Z	2		
T (K)	300	150	50
a (Å)	11.509(2)	11.18(1)	11.11(2)
b (Å)	12.673(2)	12.42(2)	12.05(3)
c (Å)	16.077(2)	16.00(2)	16.15(3)
α (deg)	70.29(1)	70.15(8)	70.20(14)
β (deg)	81.29(1)	80.34(7)	79.60(13)
γ (deg)	84.68(1)	83.76(9)	82.55(16)
V (Å^3)	2179.9	2056.8	1995.4
ρ (g·cm^{-3})	1.79(3)		
μ (cm^{-1})	11.19		
R	0.055	0.18	0.20
Rw	0.064		

Atomic positional parameters are found in Table 2 and selected bond lengths and angles in Table 3. A summary of crystal data (Table S1) and a complete listing of bond lengths (Table SII), bond angles (Table SIII), and anisotropic thermal parameters (Table SIV) are deposited as supporting information.

Low-Temperature Neutron Diffraction Data and Structure Determination. As observed in performing EPR experiments, cooling a crystal below 100 K generally resulted in the crystal breaking. Indeed, we did not succeed in collecting X-ray diffraction data during the time allowed for measurement on a low-temperature four-circle diffractometer.

Since access to our neutron facilities at the Siloe reactor in Grenoble is more flexible, we decided to perform the low-temperature structure determination on the DN4 four-circle diffractometer equipped with a three-stage cryostat and working at a 1.1189 Å wavelength using a crystal of dimensions 0.4 × 0.6 × 0.6 mm^3. A first experiment was performed at 150 K. Cell constants were derived as described for the X-ray room-temperature experiment (Table 1), and the intensities of 856 independent reflections were measured. The room-temperature positional parameters were used as starting values in the refinement model, but in order to avoid an overparametrized problem originating from the low number of measured reflections, the molecule was defined as rigid blocks to which were assigned global isotropic thermal parameters. Thus, the free radical ligand was defined as two blocks, the only varied internal parameter being the angle between the five-membered ring and the pyridyl group. Each (hexafluoroacetylacetonato)metal fragment was defined as three blocks: the copper(II) ion and the two fluorinated ligands. Using the program MXD,[24] the refinement converged to an R value of 0.18.

After several unsuccessful attempts, a crystal was cooled to 50 K. The low-temperature cell parameters were determined, and 1191 independent reflections ($(\sin\theta)/\lambda = 0.51$ Å^{-1}) were collected. Using the same rigid block scheme as described for the 150 K experiment, the refinement converged to $R = 0.20$.

Selected bond lengths and angles are displayed in Table 3, and fractional cell coordinates are found in Table SV in the supporting information.

Owing to the difficulty to cool a crystal, determination of the cell parameters between 150 and 50 K was not performed. However, powder diffraction spectra were collected in this temperature range. One gram of a powdered sample was placed in a vanadium sample holder and mounted on the DN5 multidetector powder diffractometer working at a $\lambda = 2.49$ Å wavelength. Data were recorded every 5 K in the 80–130 K temperature range. Owing to the large cell parameters and the resolution of the diffractometer, indexation using the Rietveld[25] technique was unsuccessful.

(20) Davis, M. S.; Morokuma, K.; Kreilick, R. W. *J. Am. Chem. Soc.* **1972**, *94*, 5588.
(21) Casey, R. J.; Walker, W. R. *J. Inorg. Nucl. Chem.* **1967**, *29*, 1301.
(22) Laugier, J.; Roland, G.; Emeriau, J. *J. Appl. Crystallogr.* **1989**, *22*, 431.
(23) Sheldrick, G. M. In *Crystallographic Computing 3*; Sheldrick, G. M., Kruger, C., Goddard, R., Eds.; Oxford University Press: Oxford, U.K. 1985; p 175.
(24) Wolfers, P. *J. Appl. Cryst.* **1990**, *23*, 554.
(25) Rodriguez-Carvajal, J. *Physica B* **1993**, *192*, 55.

Table 2. Fractional Coordinates ($\times 10^4$) at Room Temperature

	X	Y	Z	B_{eq}[a] (Å^2)		X	Y	Z	B_{eq}[a] (Å^2)
Cu1	905(1)	3012(1)	2301(1)	5.07	C22	3224(10)	4388(9)	−7(6)	4.95
Cu2	3709(1)	1347(1)	−1564(1)	3.51	C23	865(9)	1320(11)	−2938(6)	5.46
O3	−245(8)	2221(8)	3239(4)	5.50	C24	1660(7)	1831(8)	−2492(5)	3.56
O4	1378(7)	3853(7)	2987(4)	5.41	C25	1621(12)	2898(12)	−2731(7)	6.12
O5	61(9)	2657(9)	1483(4)	6.18	C26	2269(11)	3550(9)	−2400(6)	4.97
O6	2120(8)	3736(8)	1366(4)	6.15	C27	2169(19)	4805(13)	−2759(9)	8.64
O7	2210(6)	1081(6)	−1920(4)	4.70	C28	5051(17)	2963(11)	−4204(7)	7.36
O8	2962(8)	3140(6)	−1819(4)	5.87	C29	5086(10)	2497(9)	−3187(5)	4.50
O9	4320(7)	1791(6)	−2840(3)	4.74	C30	5873(11)	2871(8)	−2799(5)	4.62
O10	5190(6)	1764(6)	−1309(3)	4.17	C31	5861(10)	2500(8)	−1888(6)	4.23
O1	2207(7)	1488(7)	2767(4)	5.10	C32	6775(16)	2914(12)	−1488(7)	7.62
O2	5735(6)	587(6)	1299(3)	4.45	F1	−1390(14)	1461(14)	5446(4)	17.11
N2	4966(7)	968(6)	1828(4)	3.35	F2	−1175(15)	508(11)	4585(8)	15.49
N1	3286(7)	1365(7)	2540(4)	4.17	F3	−2382(8)	1911(12)	4352(6)	11.18
N3	3115(8)	786(7)	−248(4)	3.58	F4	2665(7)	4582(7)	3921(5)	7.85
C1	3815(10)	1020(8)	1853(4)	3.70	F5	1296(8)	4240(7)	5025(4)	9.21
C2	4259(9)	1496(10)	3062(6)	4.72	F6	1137(10)	5501(7)	3826(6)	9.18
C3	5372(10)	1509(9)	2446(6)	4.68	F7	10(8)	2440(12)	−552(6)	11.77
C4	3878(14)	2459(12)	3396(10)	7.21	F8	−1082(11)	1774(11)	616(6)	12.37
C5	4153(17)	324(16)	3904(8)	9.17	F9	−1223(13)	3450(14)	−117(13)	17.47
C6	5721(15)	2653(11)	1855(9)	7.01	F10	3721(7)	5049(7)	302(4)	7.40
C7	6400(11)	788(14)	2871(8)	6.90	F11	3083(10)	4914(9)	−826(4)	9.88
C8	3181(9)	738(8)	1235(5)	3.21	F12	4123(8)	3564(8)	−71(7)	10.11
C9	2147(11)	222(10)	1515(6)	4.71	F13	660(6)	210(7)	−2481(4)	7.62
C10	1558(13)	−47(11)	897(6)	6.50	F14	1527(7)	1273(8)	−3720(4)	9.13
C11	2128(11)	236(12)	48(6)	5.05	F15	−39(9)	1903(8)	−3170(7)	10.00
C12	3655(9)	1014(8)	344(5)	3.19	F16	1845(15)	5218(8)	−3549(6)	11.54
C13	−1297(13)	1531(16)	4650(8)	8.30	F17	1383(17)	5180(9)	−2185(8)	12.40
C14	−355(13)	2260(11)	4025(6)	5.87	F18	3082(16)	5297(8)	−2778(9)	13.15
C15	220(11)	2913(10)	4351(6)	5.00	F19	4267(10)	3766(11)	−4395(5)	12.61
C16	978(11)	3678(9)	3803(5)	4.71	F20	5021(13)	2301(8)	−4585(4)	13.57
C17	1520(10)	4526(9)	4159(6)	4.97	F21	6008(10)	3597(12)	−4612(4)	12.96
C18	−474(16)	2631(11)	151(7)	6.79	F22	6596(11)	4057(8)	−1726(6)	11.05
C19	402(10)	2912(10)	636(6)	4.67	F23	6636(9)	2549(8)	−628(4)	10.29
C20	1367(12)	3442(12)	180(6)	5.89	F24	7794(8)	2760(11)	−1834(6)	10.71
C21	2149(10)	3831(9)	571(5)	4.40					

[a] $B_{eq} = 8\pi^2(U11 + U22 + U33)/3$.

Table 3. Selected Bond Lengths (Å) and Angles (deg)

	300 K	150 K	50 K
Cu1–O1	2.316(8)	2.270(35)	2.404(36)
Cu1–O3	1.912(8)	1.866(30)	1.937(28)
Cu1–O4	1.932(9)	1.975(48)	2.048(50)
Cu1–O5	1.934(10)	1.941(41)	1.929(44)
Cu1–O6	1.931(8)	1.958(29)	1.898(27)
Cu2–N3	2.022(6)	2.021(28)	2.052(30)
Cu2–O2	2.384(7)	2.297(44)	2.028(50)
Cu2–O7	1.989(7)	2.045(54)	2.379(54)
Cu2–O8	2.277(7)	2.297(67)	1.942(71)
Cu2–O9	1.969(5)	1.950(46)	1.943(47)
Cu2–O10	1.969(7)	2.052(60)	2.171(53)
Cu2i–O2	2.384(7)	2.297(44)	2.028(50)
N1–O1	1.251(10)		
N2–O2	1.308(9)		
O3–Cu1–O6	176.9(4)	179.0(1.8)	173.3(1.9)
O4–Cu1–O5	159.0(4)	154.9(2.1)	161.8(2.1)
O–Cu1–O (av)	91(8)	91(18)	90(23)
O7–Cu2–O10	174.0(2)	166.7(3.0)	174.3(2.4)
O2–Cu2–O8	173.3(3)	171.2(1.8)	168.5(1.8)
N3–Cu2–O9	176.2(3)	177.3(2.2)	176.9(2.9)
O–Cu2–O (av)	90(4)	89(21)	90(23)
Cu1–O1–N1	131.3(4)	127.8(1.4)	126.2(1.3)
Cu2i–O2–N2	122.9(4)	121.3(1.2)	123.1(1.4)
C1–N1–O1	127.6(9)		
C1–N2–O2	126.5(8)		
N1–C1–N2	110.5(9)		

Specific Heat Measurements. Data were collected using an adiabatic high-resolution calorimeter precisely calibrated as previously described.[26] The sample was in the form of a 50 mg sintered pellet glued onto a sapphire plate with vacuum grease. Since thermal coupling between the sample and the thermometer was not very efficient, a slow heating rate of 0.5 K·min^{-1} was used. The temperature was sampled every 10 s and the derivative dT/dt calculated over temperature ranges of approximately 1 K to give a rms scatter much below 1%. Several measurements were performed in the 45–200 K temperature range, and the absolute error was estimated to be lower than 5%.

Results

Structural Studies. The higher than usual low-temperature R values are clearly related to the block refinement model which includes global isotropic thermal parameters. Therefore, discussion of the structural results will be restricted to qualitative comparison of chemically significant features such as ligand to metal coordination geometry whose meanings are not hampered by the low quality of the determinations at 150 and 50 K.

The room-temperature molecular structure is shown in Figure 1. The cluster is a centrosymmetric cyclic dimer comprising two nitroxide free radicals and four copper(II) ions. Among these metal ions, two are involved in the cyclic structure and are octahedrally coordinated (Cu2) while the two others are extracyclic and in a square pyramidal environment (Cu1). This description is only approximate as shown by angle values far from the ideal values of 90° and 180°. The three potential donor sites of the NIT-3Py ligand (O1, O2, N1) all are coordinated to metal ions, the pyridine nitrogen atom being linked to the intracyclic copper ion. Worth noting is the axial ligation of both the nitroxide oxygen atoms at distances O1–Cu1 = 2.316(8) Å and O2–Cu2 = 2.384(7) Å, and the equatorial binding

(26) Junod, A.; Bonjour, E.; Calemczuk, R.; Henry, J. Y.; Muller, J.; Triscone, G.; Vallier, J. C. *Physica C* **1993**, *211*, 304.

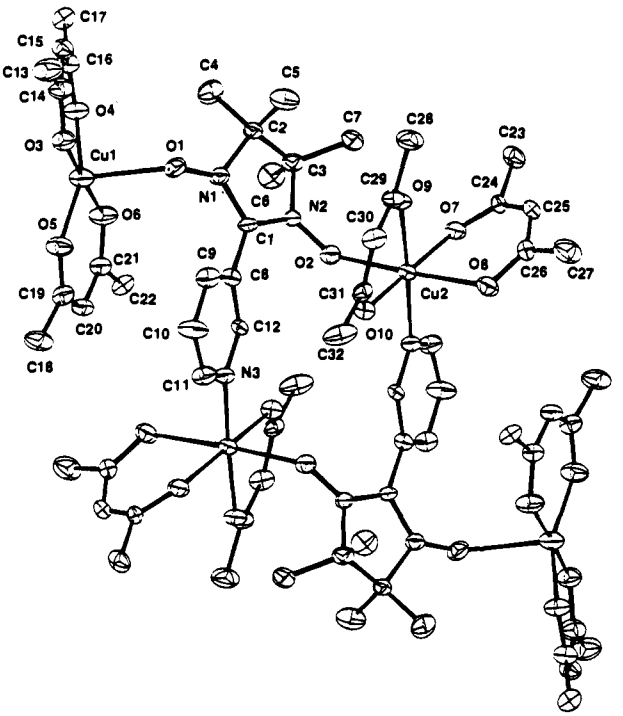

Figure 1. View of the molecular structure showing the numbering scheme. Thermal ellipsoids are drawn at the 30% probability level.

of the pyridine nitrogen (N3−Cu2 = 2.022(6) Å). The structural features of the free radical ligand are similar to those reported for several examples of uncoordinated[27−30] and coordinated[13−19] nitronyl nitroxides. Of interest, however, are the angle between the two rings (47.5(8)°) and the NO bond lengths 1.251(10) and 1.308(9) Å for the NO groups bound to Cu1 and Cu2, respectively.

At 50 K, one observes the same space group and the same cyclic dimeric structure. While the overall geometry of the complex is similar to that observed at room temperature, the coordination sphere of the intracyclic copper ions (Cu2) is subject to dramatic modifications. As shown in Figure 2, at low temperature the coordination geometry may also be approximated as octahedral, but both the nitroxyl oxygen and the pyridine nitrogen atoms are now equatorially bound. Concomitantly, one O(hfac)−Cu bond has shortened while two others have lengthened. In contrast, no drastic change is observed for Cu1 except for a weak (0.09 Å) but significant lengthening of the axial O1 (nitroxyl) binding to Cu1. Concerning the nitroxide ligand, the block refinement procedure only provides the modification (≅5°) of the angle between the two cyclic fragments (42(1)°).

Magnetic Susceptibility Studies. The temperature dependence of the product of the magnetic susceptibility with the temperature is displayed in Figure 3. Schematically, one observes two Curie law regimes. The high-temperature values (300−140 K, 2.56 emu·K·mol^{-1}, $\mu = 4.53\ \mu_B$) are very close to those expected for six independent copper(II) ions ($g > 2$) and nitroxide ligands ($g = 2$). At low temperature (70−4 K), values of χT correspond to two independent $S = 1/2$ spins (0.84 emu·K·mol^{-1}, $\mu = 2.59\ \mu_B$). In the following text, these two

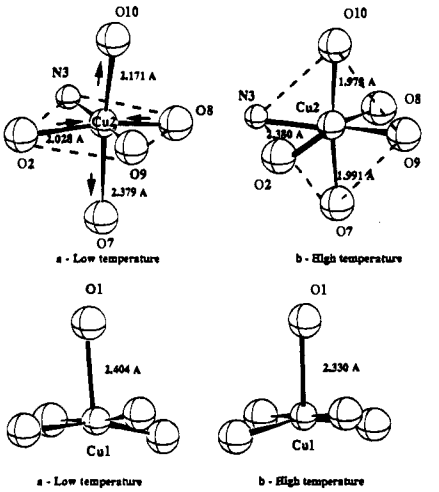

Figure 2. Intra- and extracyclic copper environments at 300 and 50 K.

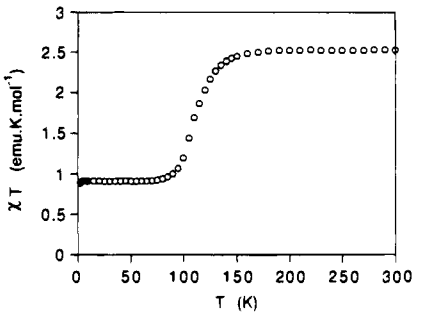

Figure 3. Temperature dependence of the product of the magnetic susceptibility with the temperature.

regimes will be referred to as "high spin" and "low spin", respectively. Between 140 and 70 K, one observes a smooth decrease of χT which corresponds to the "loss" of four spins. This decrease occurs in the same temperature range as the structural modifications; it is therefore inferred that both phenomena are strongly correlated. On increasing the temperature back to the original temperature, an identical curve is obtained, showing that within temperature uncertainties no hysteresis effect is detected.

The susceptibility data shown in Figure 3 were converted to values of the fraction of high-spin species at a given temperature. Taking the 50% point conversion to define the transformation gives a transition temperature of 110 K.

EPR Studies. Powders and crystals as well are EPR silent at room temperature except for a weak and narrow signal which is probably due to free radical and/or copper(II) ions present as an impurity. Such signals are commonly observed in antiferromagnetically exchange-coupled metal−nitroxide species.[31] However, since magnetic susceptibility measurements show that the spins are independent at room temperature, the absence of signal in this cluster is most probably the consequence of dipolar interactions or relaxation effects as previously observed in several similar clusters.[32,33] On decreasing the temperature, the powders suddenly exhibit a strong and large signal which appears below 110 K. The temperature dependence of the signal line width is the EPR parameter exhibiting the sharper variation with the temperature; it is used for determining the temperature of the signal appearance: 110 ± 1 K. Note the perfect

(27) Wong, W.; Watkins, S. F. *J. Chem. Soc., Chem. Commun.* **1973**, 888.
(28) Awaga, K.; Inabe, T.; Nagashima, U.; Maruyama, Y. *J. Chem. Soc., Chem. Commun.* **1989**, 1617.
(29) Awaga, K.; Okuno, T.; Tamaguchi, A.; Hasegawa, M.; Inabe, T.; Maruyama, Y.; Wada, N. *Phys. Rev. B* **1994**, *49*, 3975.
(30) Lanfranc de Pauthou, F.; Luneau, D.; Laugier, J.; Rey, P. *J. Am. Chem. Soc.* **1993**, *115*, 9095.
(31) Porter, L. C.; Dickman, M. H.; Doedens, R. J. *Inorg. Chem.* **1986**, *25*, 678.
(32) Richardson, P. F.; Kreilick, R. W. *J. Magn. Reson.* **1978**, *29*, 285.
(33) Luneau, D.; Rey, P.; Laugier, J.; Fries, P.; Caneschi, A.; Gatteschi, D.; Sessoli, R. *J. Am. Chem. Soc.* **1991**, *113*, 1245.

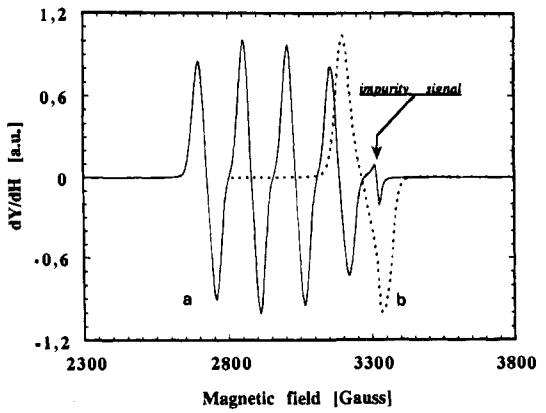

Figure 4. EPR spectra for a monocrystal at 4.2 K. Spectra a and b correspond to the maximum and minimum hyperfine splitting when the field is rotated in the $\vec{b}-\vec{a},\vec{c}$ plane.

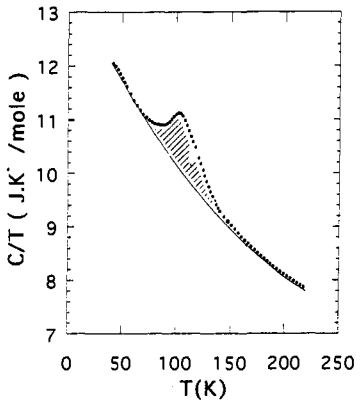

Figure 5. Temperature dependence of the specific heat (C) divided by the temperature.

agreement of this value with that corresponding to 50% conversion determined from the magnetic data.

Low-temperature spectra of a single crystal exhibit a well-resolved hyperfine pattern characteristic of a copper(II) ion in a tetragonal environment (Figure 4).[34] The crystal was oriented in such a way that rotation around the vertical axis brings the magnetic field into the $\vec{b}-\vec{a},\vec{c}$ plane which approximately contains the Cu1–O1 bond. Only one hyperfine pattern was observed for each orientation of the field and the maximum and minimum values of a_{Cu} and g_{Cu}. a_{max} = 153 Oe, g_{max} = 2.281, a_{min} = 34 Oe, and g_{min} = 2.067 are consistent with those expected for an elongated tetragonal copper(II) ion. This experiment ascertains that the only active spin carrier at low temperature is a copper(II) ion which is probably the extracyclic one, Cu1.

Specific Heat Studies. The temperature dependence of C/T is displayed in Figure 5. One observes a broad anomaly, centered at 110 K, superimposed on a large phonon contribution. Estimation of this contribution was performed by fitting the total specific heat far from 110 K with a smooth polynomial of degree 2. Substraction of this function from the total specific heat around 110 K gives a reasonable estimate of the enthalpy and entropy associated with the anomaly: ΔH = 3.6(2) kJ·mol^{-1}, ΔS = 33(1) J·K^{-1}·mol^{-1}.

The absence of hysteresis in the temperature dependence of the magnetic susceptibility, the same space group at room and low temperature, and the round shape of the heat capacity anomaly strongly suggest that the phase transition is second-order or higher.

(34) Hataway, B. J. *Coord. Chem. Rev.* **1982**, *41*, 423.

Discussion

Pyridyl-substituted nitronyl nitroxides have been recently used as ligands toward transition-metal ions[35–38] with the aim of designing three-dimensional exchange-coupled species thanks to the presence of three sites of coordination. First-row transition-metal complexes derived from the 3-pyridyl-substituted ligand are discrete compounds which have the reported cyclic centrosymmetric structure. In addition to these derivatives and depending on the starting ratio of nitroxide ligand and metal precursor, other centrosymmetric complexes in which two free radicals are equatorially bound to the metal center by their pyridyl nitrogen atom could be isolated.[39] Down to 2 K, these three-spin adducts exhibit a Curie behavior corresponding to three independent spins which shows that the 3-pyridyl group is not an efficient pathway for magnetic coupling between the free radical ligand and metal centers.

Since in the cyclic copper(II) complex under investigation the binding of the pyridyl nitrogen atom to the intracyclic copper(II) ion (Cu2) is very similar, from a magnetic point of view the compound should be considered as the sum of two independent three-spin systems (Cu1–ligand–Cu2). In each of these fragments, two copper(II) ions are bridged by a nitroxide ligand, both bindings of the nitroxyl groups being axial. Therefore, the expected magnetic properties should be those of the well-documented axially oxygen bound copper–nitroxide species.[11–17] Since large binding distances (Cu1–O1) = 2.316(8) Å and Cu2–O2 = 2.384(7) Å) in this coordination geometry result in weak metal–ligand ferromagnetic interactions (<50 cm^{-1}), an expected high-temperature value of χT should be that of six independent doublets. Indeed, the observed value down to 140 K is consistent with this scheme which would lead to a smooth increase and a finite value of χT ($\cong$3.8 emu·K·mol^{-1}, 5.5 μ_B) corresponding to the sum of two S = 3/2 spins at low temperature. In contrast, below 70 K one observes another Curie law behavior corresponding to two independent spins. This magnetic behavior is fully consistent with the single-crystal EPR spectra at low temperature which convincingly demonstrate that, below the transition, only "isolated" copper(II) ions are active. Therefore, two possibilities may account for the observed magnetic and spectroscopic properties: strong antiferromagnetic coupling or electron transfer between the metal and the free radical.

A temperature dependent redox process which would account for the disappearance of the spins and lead to a similar spin transition like magnetic behavior has been reported for metal derivatives of semiquinones.[40–42] Concerning nitroxide coordination chemistry, platinum[43,44] and manganese[45,46] complexes of the hydroxylamino reduced form have been reported, but in

(35) Richardson, P. F.; Kreilick, R. W. *Chem. Phys. Lett.* **1977**, *50*, 333.
(36) Richardson, P. F.; Kreilick, R. W. *J. Am. Chem. Soc.* **1977**, *99*, 8183.
(37) Caneschi, A.; Ferraro, F.; Gatteschi, D.; Rey, P.; Sessoli, R. *Inorg. Chem.* **1990**, *29*, 1756.
(38) Caneschi, A.; Ferraro, F.; Gatteschi, D.; Rey, P.; Sessoli, R. *Inorg. Chem.* **1990**, *29*, 4217.
(39) Lanfranc de Panthou, F. Thesis, Grenoble, 1994.
(40) Pierpont, C. G.; Larsen, S. K.; Boone, S. R. *Pure Appl. Chem.* **1988**, *60*, 1331.
(41) Pierpont, C. G.; Buchanan, R. M. *Coord. Chem. Rev.* **1981**, *38*, 45.
(42) Adams, D. M.; Dei, A.; Rheingold, A. L.; Hendrickson, D. N. *J. Am. Chem. Soc.* **1993**, *115*, 8221.
(43) Porter, C. L.; Doedens, R. J. *Acta Crystallogr.* **1985**, *C41*, 838.
(44) Dickman, M. H.; Doedens, R. J. *Inorg. Chem.* **1982**, *21*, 682.
(45) Caneschi, A.; Gatteschi, D.; Laugier, J.; Rey, P.; Zanchini, C. *Inorg. Chem.* **1989**, *28*, 1969.
(46) Carducci, M. D.; Doedens, R. J. *Inorg. Chem.* **1989**, *28*, 2492.

systems involving copper(II) and nitroxide free radicals the few known examples establish the presence of the oxidized (nitrosonium) form of the ligand.[47] In most copper(II)−nitroxide species, however, the free radical character of the ligand is well established.[10−19] In $\{[Cu(hfac)_2]_2(NIT\text{-}3Py)\}_2$, owing to the block refinement procedure, a change in the NO bond length which would have characterized an electron transfer is not available. However, such a redox process is very unlikely because at low and high temperature the overall square pyramidal and octahedral environments of the metal centers are retained.

Full understanding of the transition phenomenon comes from features of the low-temperature molecular structure. While at room temperature axial coordination of the nitroxide ligand occurs for both metal centers, at 50 K one observes an equatorial ligation of the nitroxide ligand to the intracyclic copper(II) ion (Cu2) which suggests that a decrease of χT between 140 and 70 K has to be found in the change of coordination geometry of the intracyclic metal ion (Cu2). Indeed, if as mentioned a weak metal−ligand ferromagnetic coupling is expected for the room temperature geometry, in contrast, equatorial binding is known to result in strong spin pairing.[18,19] Thus, at low temperature each intracyclic copper ion is strongly coupled with a nitroxide ligand such that only the two extracyclic metal ions are observed. This mechanism is fully consistent with the EPR results.

Further insight into the mechanism of the axial ↔ equatorial conversion comes from the calorimetry data. Although the coupling of unpaired spins carried by p and d orbitals can hardly be compared to the change of ground spin state in a transition-metal ion,[48] similarities in magnetic behavior and structural change suggest that specific-heat data could be more illustratively interpreted in the light of those obtained for spin-crossover compounds.[49−53] In Fe(II) spin-crossover complexes, for example, enthalpy and entropy changes were evaluated by heat capacity measurements to be $\Delta H = 8-14$ kJ·mol^{-1} and $\Delta S = 35-50$ J·K^{-1}·mol^{-1}.[54−57] Two major contributions to the substantial entropy gain are clearly recognized: the change in spin multiplicity and the change in the metal−ligand atom vibrational normal modes. In $\{[Cu(hfac)_2]_2(NIT\text{-}3Py)\}_2$, considering independent spins at low and high temperature,[58] the entropy change corresponding to spin multiplicity is $\Delta S_{SM} = 4R \ln 2 = 23.2$ J·K^{-1}·mol^{-1}. Evaluation of the sign and magnitude of the phonon mode contribution to the entropy gain is not as straightforward. In contrast to Fe(II) spin-crossover complexes in which the metal−ligand distances uniformly decrease by 0.15−0.20 Å in the conversion from the $^5T_2$ high-temperature form to the $^1A_1$ form at low temperature, in $\{[Cu(hfac)_2]_2(NIT\text{-}3Py)\}_2$ both lengthening and shortening of metal−ligand bond distances are observed. Qualitatively, however, one expects that the contribution to ΔS from the phonon modes must be weaker than that observed in Fe(II) spin-crossover compounds in agreement with the experimental value of ΔS (33 J·K^{-1}·mol^{-1}). Thus the main contribution to the entropy change comes from the change in spin degeneracy which is higher in the high-temperature phase than in the low-temperature phase. At the transition temperature the enthalpy and entropy changes must have the same sign, showing that the low-spin form of the compound is more stable than the high-spin one.[59] Therefore, at high temperature $T\Delta S$ brings a leading contribution to the Gibbs free energy, and the conversion from the high-spin state of the low-spin one is entropy driven.

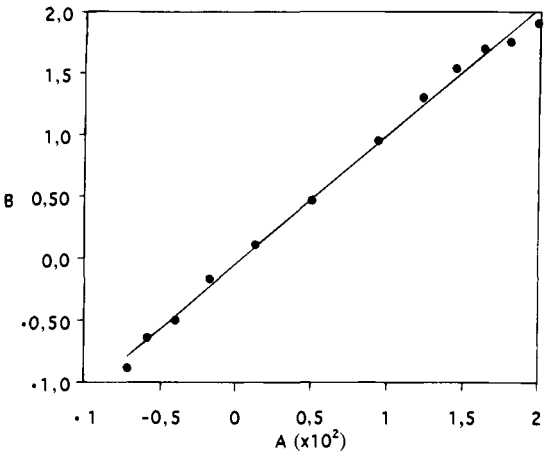

Figure 6. Graph of $A = \ln[(1 - x)/x] - \Delta H/RT + \Delta S/R$ vs $B = \gamma[(1 - 2x)/RT]$. The solid line is the best least-squares fit giving $\gamma = 1.22$ kJ·mol^{-1}.

The absence of hysteresis in the magnetic susceptibility measurements raised the question of whether the axial ↔ equatorial conversion occurs at the molecular level or is a cooperative process. The compound is dissociated in solution, and attempts to obtain a dispersion in the Zn(II) analogue were unsuccessful; therefore, magnetic measurements on "isolated" molecules were not performed. Assuming that high-spin and low-spin molecules form a regular solution at any temperature, models have been developed which afford an estimate of the intermolecular interaction in the solid state.[60,61] In Figure 6 is displayed the graph corresponding to the expression $\ln[(1 - x)/x] - \Delta H/RT + \Delta S/R = \gamma[(1 - 2x)/RT]$ in the transition temperature range 60−140 K. In this equation x is the molar fraction of high-spin molecules, γ is an interaction Gibbs free energy parameter for a coupling of the form $\Gamma = \gamma x(1 - x)$,[60] and the other symbols have their usual meaning. The observed linear dependence was a least-squares fit to give $\gamma = 1.22$ kJ·mol^{-1} (102 cm^{-1}). Since a necessary condition for observing hysteresis is $\gamma > 2RT_c$ ($T_c = 110$ K, $\gamma > 1.83$ kJ·mol^{-1} (153 cm^{-1})), this value is in agreement with the observed absence of hysteresis.

As mentioned before, this thermally induced conversion between two states of different spin value associated with metal−ligand bond changes of ca. 0.2 Å is phenomenologically similar to that observed in spin-crossover compounds. It must be stressed, however, that the mechanism of spin transition is

(47) Caneschi, A.; Laugier, J.; Rey, P. *J. Chem. Soc., Perkin Trans 1* **1987**, 1077.
(48) Ballhausen, C. J. *Introduction to Ligand Field Theory*; McGraw-Hill Inc.: New York, 1962.
(49) Cambi, L.; Cagnasso, A. *Atti. Accad. Naz. Lincei, Cl. Sci. Fis., Mat. Nat., Rend.* **1931**, *13*, 809.
(50) For reviews see: (a) Konig, E. *Coord. Chem. Rev.* **1968**, *3*, 471. (b) Goodwin, H. A. *Coord. Chem. Rev.* **1976**, *18*, 293. (c) Gutlich, P. *Struct. Bond.* **1981**, *44*, 83. (d) Konig, E. *Progr. Inorg. Chem.* **1987**, *35*, 527.
(51) Zarembowitch, J.; Kahn, O. *New J. Chem.* **1991**, *15*, 181.
(52) Kahn, O.; Krober, J.; Jay, C. *Adv. Mater.* **1992**, *4*, 718.
(53) Krober, J.; Codjovi, E.; Kahn, O.; Grolière, F.; Jay, C. *J. Am. Chem. Soc.* **1993**, *115*, 9810.
(54) Sorai, M.; Seki, S. *J. Phys. Chem. Solids* **1974**, *35*, 555.
(55) Jakobi, R.; Spiering, H.; Wiehl, E.; Gutlich, P. *Inorg. Chem.* **1988**, *27*, 1823.
(56) Sorai, M.; Maeda, Y.; Oshio, H. *J. Phys. Chem. Solids* **1990**, *51*, 941.
(57) Kulshreshtha, S. K.; Iyer, R. M.; Konig, E. *J. Phys. Chem. Solids* **1992**, *53*, 39.
(58) Calculations taking into account a metal−nitroxide interaction of +30 cm^{-1} led to the same result within a few percent.
(59) Kahn, O. *Molecular Magnetism*; VCH Publishers: New York, 1994; p 53.
(60) Slichter, C. P.; Drickamer, H. G. *J. Chem. Phys.* **1972**, *56*, 2142.
(61) Kahn, O.; Launay, J. P. *Chemtronics* **1988**, *3*, 140.

essentially different in both types of complexes. Spin crossover is crystal field dependent and occurs without symmetry change while in $\{[Cu(hfac)_2]_2(NIT\text{-}3Py)\}_2$ the change in spin multiplicity is associated with a Jahn−Teller instability of the octahedral copper(II) ion and a switch of the magnetic orbital.

Concluding Comments. A complex of a nitronyl nitroxide with $Cu(hfac)_2$ which undergoes conversion between two states of different spin multiplicity with temperature has been characterized. The phase transition involves a change of the free radical coordination geometry from axial to equatorial.

Other copper(II)−nitroxide complexes exhibiting the same phenomenon will be reported. As for spin-crossover complexes, gradual or abrupt transformations involving hysteresis or not are observed. In this respect, these copper(II) derivatives of nitroxide free radicals may be considered as "spin-transition" compounds of a new type.

Acknowledgment. This work was supported by the CEA, the CNRS, the HCM (CHRX CT 920080), and INTAS (94-3508) programs of the European Community.

Supporting Information Available: Summary of crystal data (Table S1) and listings of bond lengths (Table S2), bond angles (Table S3), anisotropic thermal parameters (Table SV) at 300 K, and fractional cell coordinates (Table SVI) at 50 K (10 pages); listing of calculated and observed structure factors (13 pages). This material is contained in many libraries on microfiche, immediately follows this article in the microfilm version of the journal, can be ordered from the ACS, and can be downloaded from the Internet; see any current masthead page for ordering information and Internet access instructions.

JA952479E